Korean J. Chem. Eng., 33(3), 1059-1069 (2016)
DOI: 10.1007/s11814-015-0220-x

pISSN: 0256-1115
eISSN: 1975-7220

Combined operation of outlet streams swing with partial-feed in a simulated moving bed

Kyung-Min Kim, Ji-Yeon Song, and Chang-Ha Lee†

Department of Chemical and Biomolecular Engineering, Yonsei University,
50, Yonsei-ro, Seodaemun-gu, Seoul 03722, Korea
(*Received 18 August 2015 • accepted 17 October 2015*)

Abstract−The operational strategy of outlet streams swing (OSS) operation combined with partial-feed (PF) operation, OSS-PF, was studied under the constraint of maximum allowable pressure and flow-rate. Its separation performance and dynamic behavior were compared with those of OSS operation and conventional simulated moving bed (SMB) chromatography. During OSS-PF operation, the switching period consisted of two steps; raffinate was produced during the closed condition of extract node and feed node in the first step, while extracts were produced and feeds were injected during the closed condition of raffinate node in the second step. As a result, OSS-PF operation could be performed under the allowable maximum flow-rate in the corresponding conventional SMB without generating an additional pressure drop at the adsorbent bed, which was different from OSS operation. OSS-PF operation successfully improved the separation performance of the conventional SMB with regard to extract purity, raffinate recovery and raffinate productivity with equivalent eluent consumption. The step ratio during a switching period worked as one of important operating variables in separation performance. The dynamic behavior of OSS-PF operation was analyzed and compared with that of OSS and conventional SMB using simulated concentration profiles in the fluid phase.

Keywords: Simulated Moving Bed (SMB), Outlet Streams Swing (OSS), Partial-feed, Pressure Drop

INTRODUCTION

The simulated moving bed (SMB) process is a multicolumn chromatographic separation process. Compared to batch chromatography, greater productivity and lower solvent consumption can be achieved during SMB operation, primarily due to countercurrent flow configuration. Therefore, SMB technology has been applied to hydrocarbon and sugar separations since the 1960s [1-3], and its application is being further extended to fine chemicals and pharmaceuticals [4-6].

A four-zone SMB with one or two columns in each zone, as shown in Fig. 1(a), has been the most widely adopted configuration (1-1-1-1 or 2-2-2-2 configuration), with each zone playing a specific role with regard to production and separation. Countercurrent movement of the adsorbent bed is simulated by periodically shifting the inlet and outlet nodes to the direction of the flow. This shift of each node is called a 'switch,' and the time interval between two consecutive switches is called 'switch time' or 'switching period.'

The raw solution is fed into a feed node between zones II and III in an SMB unit. Raffinate component (B) with a lower adsorption affinity to the adsorbent is more weakly retained and is transported via fluid flow toward a raffinate node, while species with greater retention, such as extract component (A), are strongly adsorbed and transported to an extract node via movement of the adsorbent bed. In zone I, the fluid flow rate is adjusted such that the strongly retained product (A) can be desorbed from the adsorbent phase via eluent (desorbent: D), allowing for the pure adsorbent to be recycled into zone IV. In zone IV, the fluid flow rate is sufficiently low to allow for the adsorption of raffinate component (B).

During conventional SMB operation, the raffinate and extract concentration profiles at each product node are formed during switching periods (Figs. 1(b) and (c)). The impurity (extract component) at the raffinate product node elutes during the last stage of the switching period, while the raffinate component is presented as an impurity during the initial switching period of the extract product node. As a result, to improve the operational separation performance of a conventional SMB, various strategies have been developed to reduce the impurity profile of each product node.

A partial-discard operation simply discards the low-purity components during a switching period to satisfy the product purity requirement [7]. The discarded components are recycled within the feed node during recycling partial-discard operation because the purity is always higher than the feed [8]. The impurity can also be handled via control of the feed concentration during ModiCon operation [9]. Additionally, the impurity profile of a product node can be shifted outside the product node by supplying a certain portion of the product during feeding time of the backfill-SMB operation [10]. In the FeedCol operation, a small column is added prior to the feed node, and the concentrated pulse feed is pre-separated [11].

Alternatively, the impurity profile at each product node can be shifted by controlling the feed flow-rate or product flow-rate. The impurity was successfully decreased by varying the feed flow-rate

†To whom correspondence should be addressed.
E-mail: leech@yonsei.ac.kr

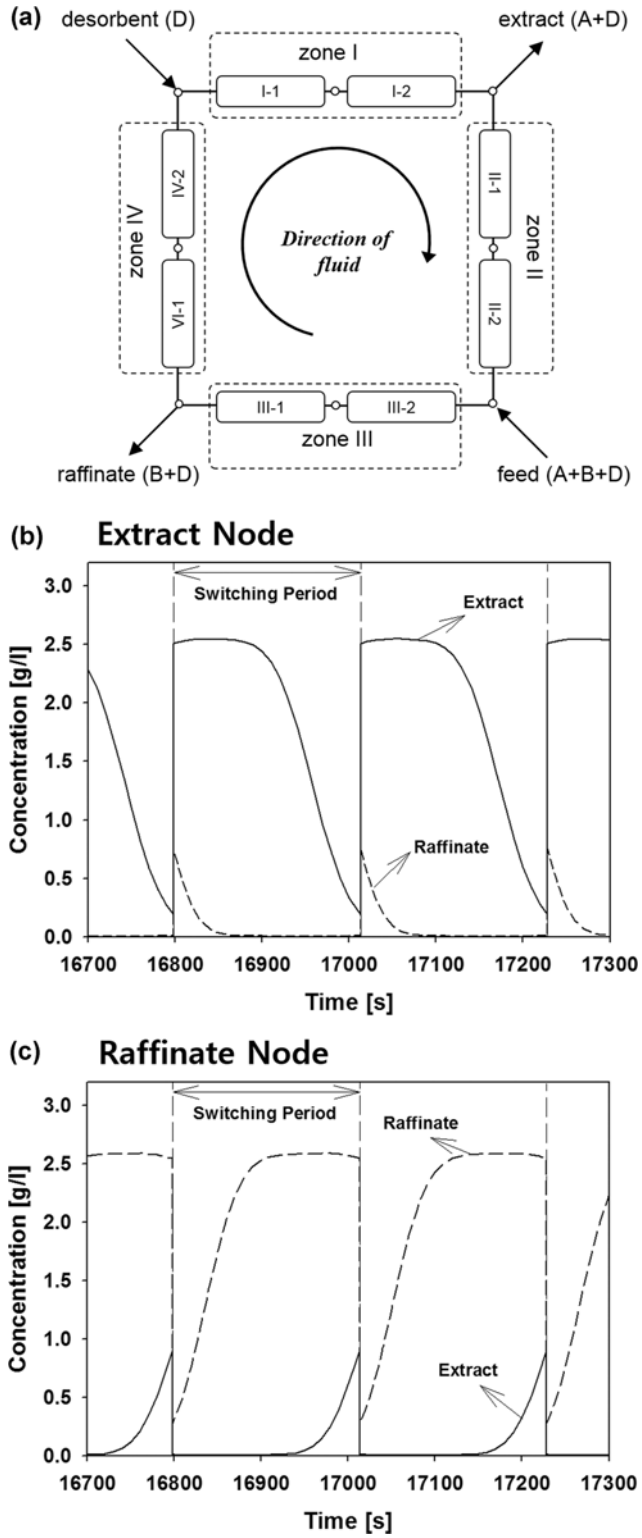

Fig. 1. (a) Scheme of conventional SMB operation with four zones; and typical concentration profiles in a conventional SMB: (b) Extract node and (c) Raffinate node.

during a switching period in partial-feed operation [12,13]. During outlet streams swing (OSS) operation, the purity can be improved by decreasing the product flow-rate as propagation of the contaminated profile is delayed from the product node [14]. Changing the flow-rate at the product node has also been implemented for three-zone SMB using three-port operation [15] and for five-zone SMB to separate ternary mixture [16]; the separation performance was significantly enhanced. A combination of product flow-rate control and feed flow-rate control was also suggested in the previous studies, but the approach and objective of each study were different. PF-PCE_2 strategy was developed for collecting the intermediate-affinity solute in five-zone SMB, resulting in high separation performance in ternary mixture [17]. Recently, OSSv strategy was suggested as one of the optimized structures by multi-objective optimization using a superstructure formulation to maximize feed throughput and minimize desorbent usage [18]. However, these SMB operational strategies using flow-rate control are limited by applied pressure and flow-rate in each zone because overly harsh conditions lead to deterioration of the adsorbents and columns. If the bed porosity is changed or the adsorbents are contaminated, separation performance of the SMB is considerably decreased due to column malfunction [19]. Therefore, the SMB operational strategy using flow-rate control requires development under the constraint of maximum allowable pressure or flow-rate.

In this study, the combined operational strategy of OSS (product flow-rate control) and PF operations (partial-feed: feed flow-rate control), named OSS-PF (outlet streams swing with partial-feed), was designed and applied to a four-zone SMB with one column per zone (1-1-1-1). Therefore, this study is an extension of the studies using flow-rate control strategies in SMB operation. However, since the OSS-PF study was carried out under the constraint of maximum allowable pressure and flow-rate for an SMB unit, the major concern of this study was to investigate the effect of flow-rate control on separation under a pressure drop constraint. As a representative case, a binary mixture with a linear isotherm was selected to demonstrate improvements in efficiency for the developed OSS-PF during a simulation study. Four performance parameters (purity, recovery, productivity and eluent consumption) and dynamic characteristics of the OSS-PF were compared with those of the corresponding conventional SMB and OSS operations. The separation performance was compared under the same throughput of feed within a switching period regardless of operating modes.

THEORY

1. Principle of Outlet Streams Swing and Partial-feed Operation

Fig. 2 shows the OSS and PF operations of the four-zone SMB. During OSS operation (Fig. 2(a)), the switching period was divided into two steps, and the flow-rate of the product outlet port could be changed with a fixed amount of withdrawn product. If a low flow-rate of extract and high flow-rate of raffinate were used during the first step with a high flow-rate of extract and low flow-rate of raffinate during the second step, the canonical name "*OSS raffinate-extract*" was assigned to the system (Fig. 2(a)). Otherwise, reverse flow-rate control at the product node was referred to as "*OSS extract-raffinate*."

During extreme operation, maximum purity of both products from the OSS raffinate-extract SMB could be achieved by closing one product port while the other generates product. This is due to

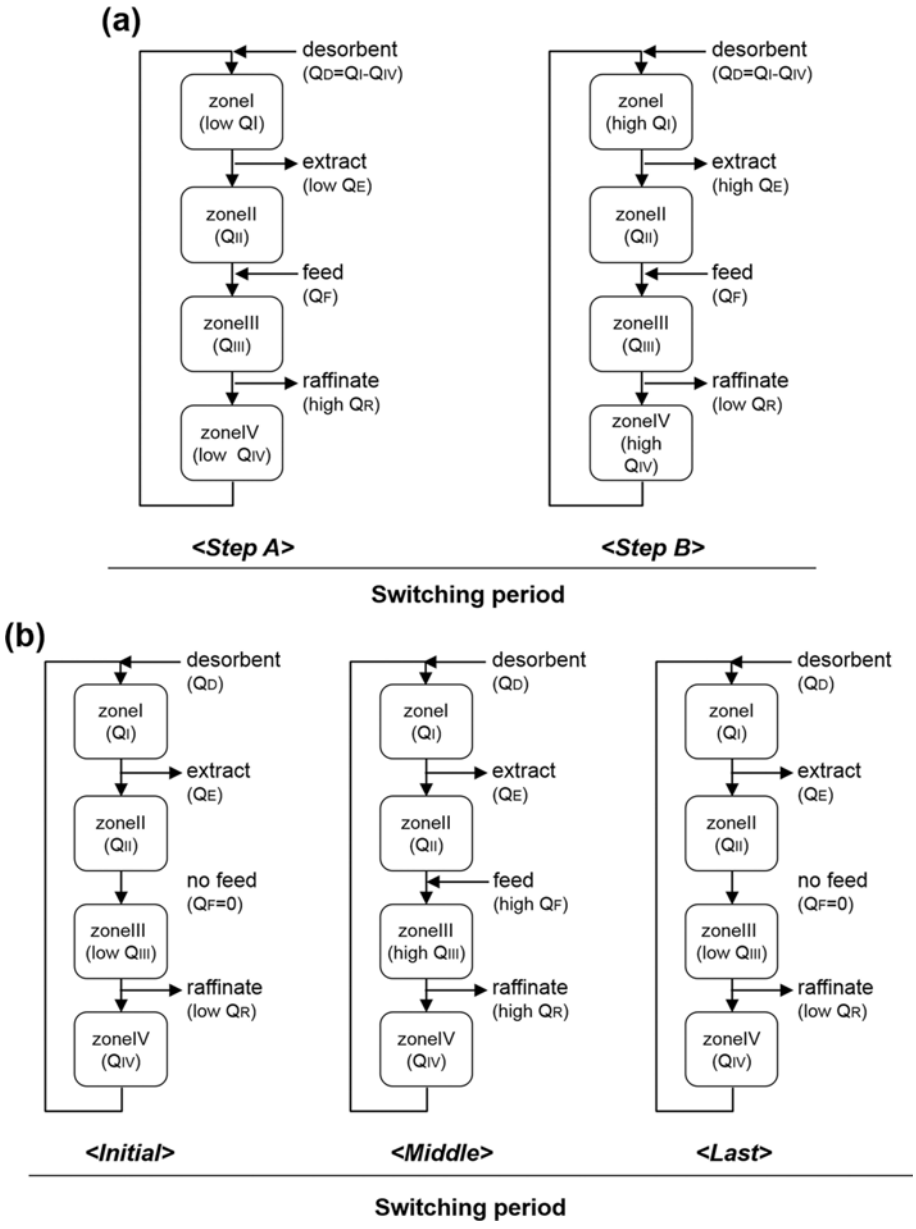

Fig. 2. Principle of (a) Outlet Streams Swing (OSS) operation and (b) Partial-feed operation.

contaminant propagation when one product port is closed during a switching period. To compare the results of the developed OSS-PF strategy, extreme OSS raffinate-extract operational cases were studied, in which complete closure of the extract port occurred during raffinate production in the first step, and complete closure of the raffinate port occurred during extract production in the second step.

During OSS operation, variations in extract and raffinate flow-rates were made by controlling the flow-rate of zones I and IV with fixed flow-rates of zones II and III. Therefore, as shown in step A of Fig. 2(a), the low flow-rate of the extract port was achieved via a low flow-rate in zone I with a fixed flow-rate in zone II. On the other hand, a large quantity of raffinate was withdrawn when the flow-rate of zone IV was decreased with a fixed flow-rate of zone III (Fig. 3(a)). The opposite operational case is illustrated in step B. The quantity of fluid passing through zones I and IV during the entire switching period was the same as that observed for a corresponding conventional SMB.

During PF (partial-feed) operation of the OSS-PF, the feed flow-rate exhibited a discontinuous pulse flow during the switching period (Fig. 2(b)). Each switching period was divided into three intervals, and the feed was injected during the middle interval. Due to variations in the feed flow-rate, the flow rates of zone III and the raffinate node were changed to the fixed flow-rate of zone IV. The amount of feed during a switching period also remained the same as that of a corresponding conventional SMB.

2. Design of Operating Parameters with Maximum Flow-rate Limits

Conventional SMB processes have five degrees of freedom: four internal flow-rates, Q_j (j=I, II, III, IV), and the switching period,

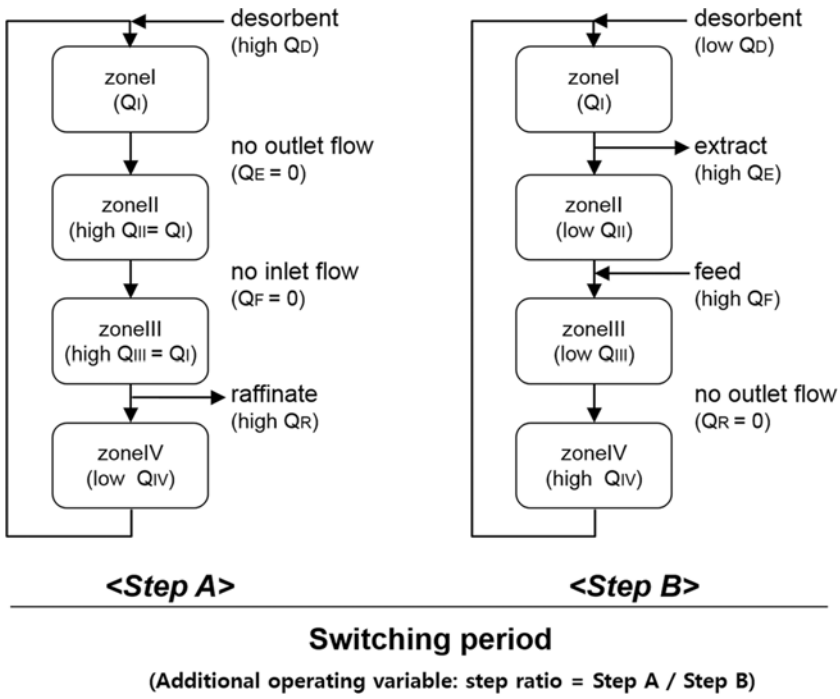

Fig. 3. Principle of Outlet Streams Swing with Partial-feed (OSS-PF) operation.

t_{sw}. To determine the operating parameters, constraints on the four flow-rate ratios, m_j, were provided from triangle theory [20] as follows:

$$m_j = \frac{Q_j t_{SW} - V\varepsilon}{V(1-\varepsilon)} \quad (1)$$

For a linear isotherm:

$$H_A < m_1 \quad (2)$$

$$H_B < m_2 < m_3 < H_A \quad (3)$$

$$m_4 < H_B \quad (4)$$

where Q_j is the volumetric flow-rate in zone j, V and ε are the column volume and total porosity, respectively, and H_i is the Henry constant of the ith component. To interpret the process, one more constraint is needed, but the value varies on a case-by-case basis.

Typically, chromatographic processes have a specific limitation on the maximum flow-rate within a column because violating the maximum allowable flow-rate would damage the packed adsorbents and lead to degradation in separation performance [19]. Therefore, limiting the maximum allowable flow-rate could be an additional constraint in designing the operating parameters for OSS-PF operation. The maximum flow-rate used in this study will be defined in a later section.

3. Design of Operating Conditions for Outlet Streams Swing with Partial-feed Operation under Flow-rate Limits

The flow-rate in zone I is usually the maximum flow-rate in a conventional SMB based on Eqs. (1)-(4), implying the maximum allowable flow-rate for a column. Therefore, the flow-rate of zone I was also defined as the maximum value when OSS-PF operation was applied to the corresponding SMB process.

As shown in Fig. 3, in the first step, the flow-rate of zone II was the same as that of zone I without outlet flow of the extract node. The feed node had to be subsequently closed naturally so as not to violate the maximum allowable flow-rate in zone III. The raffinate product was collected with a high flow-rate during the first step. Additionally, the feed with a higher flow-rate than experienced with conventional SMB was injected during the second step in order to apply the same feed amount within the reduced time period during the switching period as with a conventional SMB. The extract product was collected with a high flow-rate, while the raffinate outlet stream was closed during the second step. Although four inlet/outlet nodes and internal flow-rates varied over a switching period in OSS-PF operation, the average flow-rates during a switching period in the OSS-PF operation were the same as those in conventional SMB.

During OSS-PF operation, the step ratio (θ), which is the time fraction of step A during an entire switching period, was defined to determine the time duration of each step. Thus, the time durations of step A and step B can be represented by $\theta \cdot t_{sw}$ and $(1-\theta) \cdot t_{sw}$, respectively. The step ratio range could be calculated under flow-rate constraints, which are presented in the following section. In this study, limitation of the maximum allowable flow-rate was considered to be an additional constraint. This implied that the corresponding maximum pressure drop in an adsorbent column was limited. In this case, the step ratio of OSS-PF operation was fixed where the total fluid flow during OSS-PF operation was the same as that of a corresponding conventional SMB.

MATHEMATICAL MODELS

1. Column and Node Models

The OSS-PF and conventional SMB operations were obtained by combining the single-column model with the mass balance for

each node. The column model using the equilibrium-dispersive model for a binary system is [21]:

$$\frac{\partial C_{i,j}}{\partial t}+u_j\frac{\partial C_{i,j}}{\partial z}+\frac{1-\varepsilon_t}{\varepsilon_t}\frac{\partial q^*_{i,j}}{\partial t}=D_L\frac{\partial^2 C_{i,j}}{\partial z^2},\quad D_L=\frac{uL}{2N} \tag{5}$$

$$\text{at } t=0:\ C_{i,j}=0,\ q_{i,j}=0 \qquad \text{for } 0<z<L \tag{6}$$

$$z=0:\ C_{i,j}=C^{in}_{i,j} \qquad \text{for } 0\le t \tag{7}$$

where $C_{i,j}$ is the liquid phase concentration of component i (i=A and B) in column j, $C^{in}_{i,j}$ is the concentration of component i at the inlet of a zone, $q^*_{i,j}$ is the solid phase concentration of component i in equilibrium with the fluid phase, u_j is the interstitial velocity of the liquid-phase, ε_t is the overall void fraction, L is the column length, N is the number of theoretical plates in the column, and D_L is the axial dispersion coefficient, accounting for the column efficiency. The subscript i indicates the solute, while j represents the column number (j=I, II, III and IV). In this study, the feed concentration was 3 g/L for both components and N was 80 for both components assuming the low efficiency of columns [21]. The liquid phase concentration is the mass of adsorbate in the unit volume of liquid phase and the solid phase concentration is the mass of adsorbed amount in the unit volume of solid phase.

A linear adsorption equilibrium isotherm was assumed between the liquid and solid phases:

$$q^*_i=H_iC_i \tag{8}$$

Configurations of the conventional SMB, OSS, and OSS-PF operations (Figs. 1(a), 2(a) and 3) were designed using the following mass balance equations for each node:

Desorbent node:

$$Q_{IV}+Q_D=Q_I \tag{9}$$

$$C^{out}_{i,IV}Q_{IV}=C^{in}_{i,I}Q_I \tag{10}$$

Extract node:

$$Q_I-Q_{II}=Q_E \tag{11}$$

$$C^{out}_{i,I}=C^{in}_{i,II}=C_{i,E} \tag{12}$$

Feed node:

$$Q_{II}+Q_F=Q_{III} \tag{13}$$

$$C^{out}_{i,II}Q_{II}+C_{i,F}Q_F=C^{in}_{i,III}Q_{III} \tag{14}$$

Raffinate node:

$$Q_{III}-Q_{IV}=Q_R \tag{15}$$

$$C^{out}_{i,III}=C^{in}_{i,IV}=C_{i,R} \tag{16}$$

For OSS and OSS-PF operations:

$$\text{(Extract) } Q_{E,\,Step\,A}=0,\quad Q_{E,\,Step\,B}=\frac{Q_E}{(1-\theta)} \tag{17}$$

$$\text{(Raffinate) } Q_{R,\,Step\,A}=\frac{Q_R}{\theta},\quad Q_{R,\,Step\,B}=0 \tag{18}$$

For OSS-PF operation:

$$\text{(Feed) } Q_{F,\,Step\,A}=0,\quad Q_{F,\,Step\,B}=\frac{Q_F}{(1-\theta)} \tag{19}$$

where the superscript "out" refers to the outlet stream of a column, and the subscripts "Step A" and "Step B" refer to the first and second steps, respectively, with regard to OSS and OSS-PF operations.

2. Process Performance Parameters

The results of each operation were compared in terms of purity, recovery, and productivity, defined as follows:

Major product concentration [g/L]:

$$\text{(Extract) } \overline{C}_{A,E};\qquad \text{(Raffinate) } \overline{C}_{B,R} \tag{20}$$

Purity [%]:

$$\text{(Extract) } \frac{\overline{C}_{A,E}}{\overline{C}_{A,E}+\overline{C}_{B,E}}\times 100;\qquad \text{(Raffinate) } \frac{\overline{C}_{B,R}}{\overline{C}_{A,R}+\overline{C}_{B,R}}\times 100 \tag{21}$$

Recovery [%]:

$$\text{(Extract) } \frac{Q_E\overline{C}_{A,E}}{Q_FC_{A,F}}\times 100;\qquad \text{(Raffinate) } \frac{Q_R\overline{C}_{B,R}}{Q_FC_{B,F}}\times 100 \tag{22}$$

Productivity [g/(hr L)]:

$$\text{(Extract) } \frac{Q_E\overline{C}_{A,E}}{N_{column}(1-\varepsilon)V};\qquad \text{(Raffinate) } \frac{Q_R\overline{C}_{B,R}}{N_{column}(1-\varepsilon)V} \tag{23}$$

Eleunt Consumption [L/g]:

$$\text{(Extract) } \frac{Q_D+Q_F}{Q_E\overline{C}_{A,E}};\qquad \text{(Raffinate) } \frac{Q_D+Q_F}{Q_R\overline{C}_{B,R}}; \tag{24}$$

where N_{column} represents the number of columns. Productivity here was expressed as the product mass per time and adsorbent volume [15,22] instead of adsorbent mass [2].

3. Simulation Design

The system and isotherm parameters used in the simulation study are presented in Table 1. The system was assumed as a typical low-pressure SMB system and the pressure limit of the system was fixed at 24 bar [23]. Maximum allowable total flow-rate was calculated by the following Ergun equation which has been widely used to calculate pressure drop in a packed bed [24,25].

$$\frac{\Delta P_j}{L}=150\frac{\mu u_j}{D_p^2}\left(\frac{1-\varepsilon_e}{\varepsilon_e}\right)^2+\frac{7}{4}\frac{\rho u_j^2}{D_p}\left(\frac{1-\varepsilon_e}{\varepsilon_e}\right) \tag{25}$$

$$\Delta P_{total}=\sum_{j=I}^{IV}\Delta P_j \tag{26}$$

Table 1. System parameters for conventional SMB, OSS and OSS-PF operations

System parameters	
Column diameter, D [cm]	1
Column length, L [cm]	20
Interparticle porosity, ε_b [-]	0.4
Total porosity, ε_t [-]	0.64
Particle size, D_p [μm]	15
Fluid viscosity, μ [Pa s]	0.000545 (methanol)
Fluid density, ρ [g cm^{-3}]	0.7918 (methanol)
The number of plate, N [-]	80
Linear isotherm coefficients and selectivity	
H_A (extract component) [-]	3
H_B (raffinate component) [-]	2
Selectivity [-]	1.5

Table 2. Operating parameters of conventional SMB, OSS and OSS-PF operations

Operating mode		Flow-rate [ml/min]								θ [-]
		Q_I	Q_{II}	Q_{III}	Q_{IV}	Q_D	Q_E	Q_F	Q_R	
SMB		8.00	6.11	7.37	5.63	2.36	1.89	1.26	1.73	-
OSS	Step A	6.11	6.11	7.37	3.90	2.21	0.00	1.26	3.47	0.5
	Step B	9.89	6.11	7.37	7.37	2.52	3.78	1.26	0.00	
OSS-PF1	Step A	8.00	8.00	8.00	1.07	6.93	0.00	0.00	6.93	0.25
	Step B	8.00	5.48	7.16	7.16	0.84	2.52	1.68	0.00	
OSS-PF2	Step A	8.00	8.00	8.00	3.12	4.88	0.00	0.00	4.88	0.355
	Step B	8.00	5.07	7.02	7.02	0.98	2.93	1.95	0.00	
OSS-PF3	Step A	8.00	8.00	8.00	4.53	3.47	0.00	0.00	3.47	0.5
	Step B	8.00	4.22	6.74	6.74	1.26	3.78	2.52	0.00	
OSS-PF4	Step A	8.00	8.00	8.00	5.69	2.31	0.00	0.00	2.31	0.75
	Step B	8.00	0.44	5.48	5.48	2.52	7.56	5.04	0.00	

Switching time is 3.59 min
Feed concentration is 3 g/L for both components

In the above equations, ΔP_j is the pressure drop in zone j (j=I, II, III and IV), μ is the fluid viscosity, ρ is the fluid density, and u_j is the interstitial fluid velocity in zone j. L is the column length and ε_e is the interparticle porosity. The total pressure drop, ΔP_{total} is calculated from (26), as a summation of the pressure drops in all zones. ε_e was 0.4 as a typical interparticle porosity [25]. And the properties of methanol, a typical desorbent for chromatography system [23], were used for the calculation of pressure drop.

In the simulation, the flow-rate of zone I was set to 8 ml/min (6.1 m/h in linear velocity) and the total flow-rate was 27.12 ml/min (20.7 m/h in linear velocity) to satisfy the maximum allowable total pressure limit (24 bar). The required parameters for the calculation of pressure drop using (25) and (26) are listed in Table 1. The operating parameters for the conventional SMB in Table 2 were determined inside the complete separation region (triangle theory) in Fig. 4. m_j in the Fig. 4 is the dimensionless flow-rate ratio of zone j defined as the ratio between the net fluid flow rate and net solid flow rate [2].

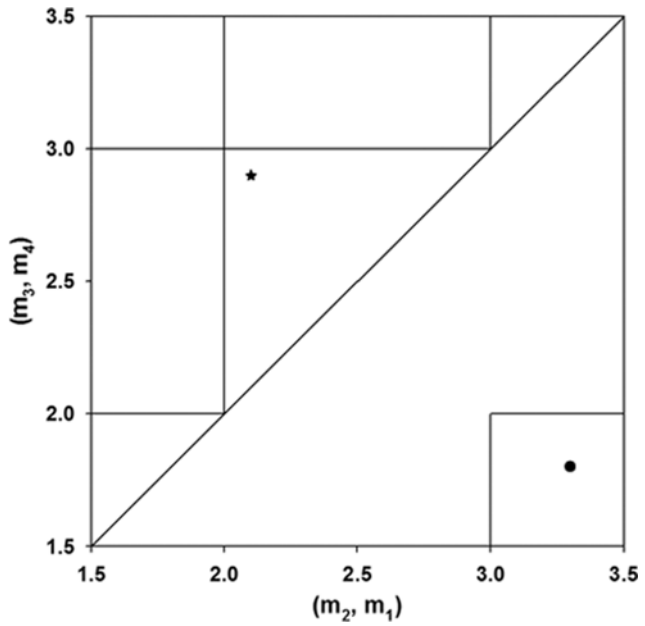

Fig. 4. Operating point in the complete separation region.

The step ratios for OSS and OSS-PF operations were determined using the following criteria:

For OSS operation:

$$Q_{R,\,Step\,A} \leq Q_{III,\,Step\,A} \quad (27)$$

For OSS-PF operation:

Maximum flow-rate limits for raffinate and extract

$$Q_{R,\,Step\,A} \leq Q_{III,\,Step\,A} \quad (28)$$

$$Q_{E,\,Step\,B} \leq Q_{I,\,Step\,B} \quad (29)$$

Maximum flow-rate limit for a system fixed according to equations

$$Q_{max} = Q_{I,\,Step\,A} + Q_{II,\,Step\,A} + Q_{III,\,Step\,A} + Q_{IV,\,Step\,A} = Q_{I,\,Step\,B} + Q_{II,\,Step\,B} + Q_{III,\,Step\,B} + Q_{IV,\,Step\,B} \quad (30)$$

From Eqs. (17), (18), and (27), the range of the step ratio for OSS operation was $0.235 \leq \theta_{OSS}$. Thus, the value was set to 0.5. From Eqs. (17)-(19), (28), and (29), the step ratio of OSS-PF operation yielded a range of $0.216 \leq \theta_{OSS\text{-}PF} \leq 0.843$. In this study, three step ratios (0.25, 0.5, and 0.75) within the aforementioned range were arbitrarily chosen to elucidate the effect of step ratio on the performance parameters. Therefore, the total flow-rate at the selected operating point (Fig. 4) in the conventional SMB was fixed to 27.12 ml/min at a switching time of 1.25 min. Naturally, flow-rate summation in each zone under OSS-PF operation was likewise set based on the conventional SMB, $Q_{max}=Q_{sum}$=27.12 ml/min; hence, the step ratio was determined by using Eqs. (28)-(30) ($\theta_{OSS\text{-}PF}$=0.355). This condition implied that the sum of the flow-rates in all zones during step A was the same as that observed for step B within a switching period. On the other hand, the flow-rate in each step was different from 27.12 ml/min when using the other step ratio conditions. Although the flow-rates between the two steps, A and B, were also different, the total flow-rate during switching remained 27.12 ml/

Table 3. Results of the conventional SMB, OSS and OSS-PF operations

Operating mode	Purity [%]		Recovery [%]		Productivity [g/L·hr]		Eluent consumption [L/g]	
	Ext	Raf	Ext	Raf	Ext	Raf	Ext	Raf
SMB	96.4	95.0	95.0	96.4	9.52	9.67	1.01	0.99
OSS	98.8	98.2	98.2	98.8	9.85	9.91	0.98	0.97
OSS-PF1	98.9	97.8	97.6	98.9	9.79	9.92	0.98	0.97
OSS-PF2	99.2	98.0	97.9	99.2	9.82	9.95	0.98	0.97
OSS-PF3	98.9	97.8	97.6	98.9	9.79	9.92	0.98	0.97
OSS-PF4	99.3	97.9	97.8	99.3	9.80	9.96	0.98	0.97

min regardless of step ratio. The separation performance at four different step ratios was evaluated in the study, and the operating parameters for each operation are listed in Table 2. All simulated results were obtained by solving the mathematical models using gPROMS ModelBuilder. Centered finite difference method (CFDM) was used with 400 discretization for an adsorbent bed.

RESULTS AND DISCUSSION

1. Separation Performance of Outlet Streams Swing with Partial-feed Operation

At the operating point specified in Fig. 4 and Table 2, the separation performance parameters for conventional, OSS, and OSS-PF SMB operations were evaluated, and the results are listed in Table 3. All performance parameters (purity, recovery, productivity and eluent consumption) of both products under OSS and OSS-PF operations were simultaneously improved from those under conventional SMB. Compared to OSS operation, OSS-PF operation was advantageous with regard to extract purity but disadvantageous with regard to raffinate purity. In terms of recovery, the results were contrary to those of purity for both products. Although the difference in purity between OSS and OSS-PF operation was small, this difference functions as a critical criterion for some fine chemicals and pharmaceuticals. The flow-rate (9.89 ml/min) in zone I under OSS operation exceeded the maximum allowable flow-rate (8 ml/min), as shown in Table 2. This result implied that OSS operation could lead to column damage from long-term operation, although the separation performance was higher than that observed under conventional SMB operation. On the other hand, OSS-PF operation could be successfully designed to satisfy the maximum flow-rate constraint in each zone, with improved separation performance.

Fig. 5 presents the internal concentration profiles of the conventional SMB and OSS-PF3 (at $\theta_{OSS\text{-}PF}$=0.5) during a steady-state cycle. Compared to the conventional SMB, the concentration of each product component at each product node (extract component near 20 cm and raffinate component near 60 cm) increased, and the concentration profile was expanded under zone I or IV. This result could be attributed to the product being withdrawn only in a corresponding step (step A or B) for a fixed step ratio (in this case, $\theta_{OSS\text{-}PF}$=0.5) during a switching period. More specifically, compared to the internal profiles of the conventional SMB, the rear extract profile during step A shifted beyond the left side of zone I (0-20 cm) and penetrated into zone IV. The front raffinate profile during step B shifted beyond the right side of zone IV (60-80 cm) and penetrated into

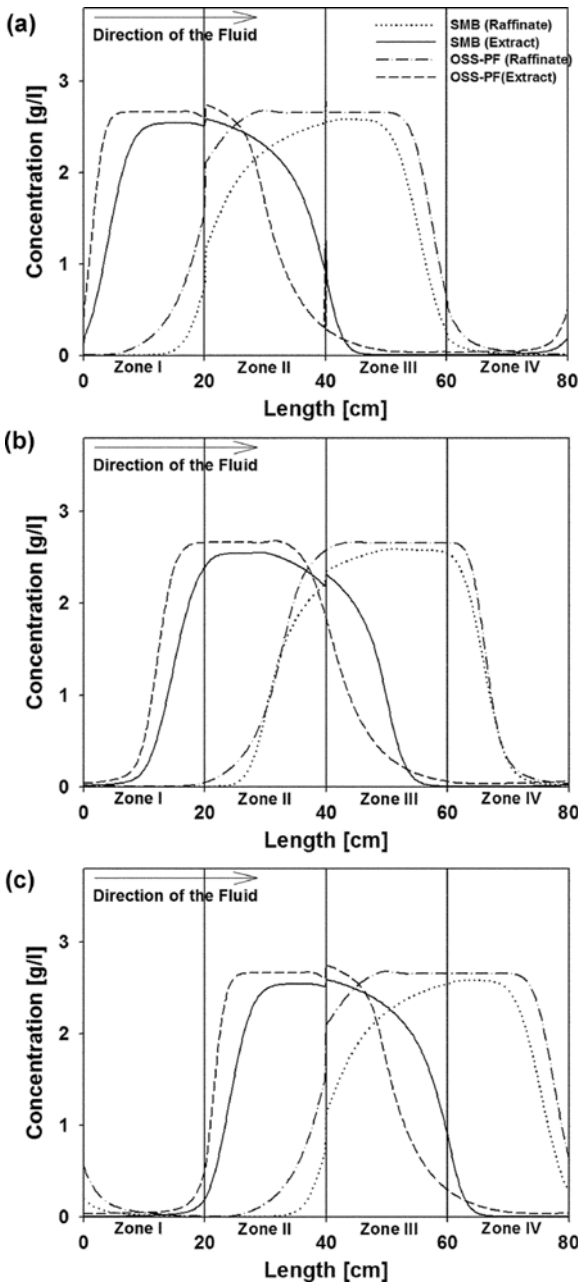

Fig. 5. Internal concentration profiles of the conventional SMB and OSS-PF operation ($\theta_{OSS\text{-}PF}$=0.5) at the (a) beginning of the switching period, (b) middle of the switching period, and (c) end of the switching period.

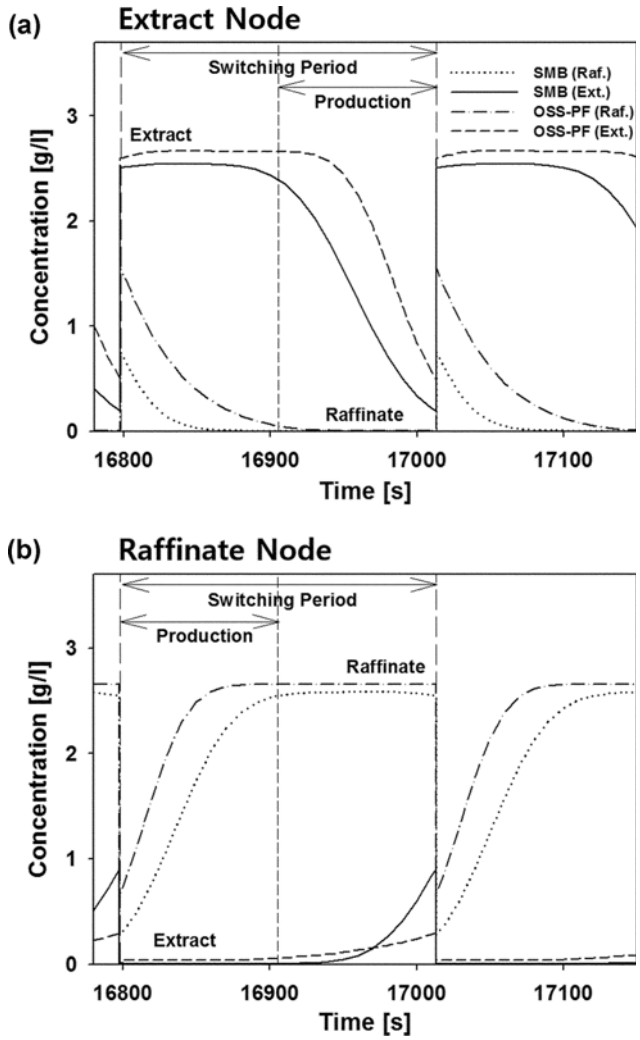

Fig. 6. Product concentration profiles of conventional SMB and OSS-PF operation ($\theta_{OSS\text{-}PF}$=0.5) at (a) extract node and (b) raffinate node.

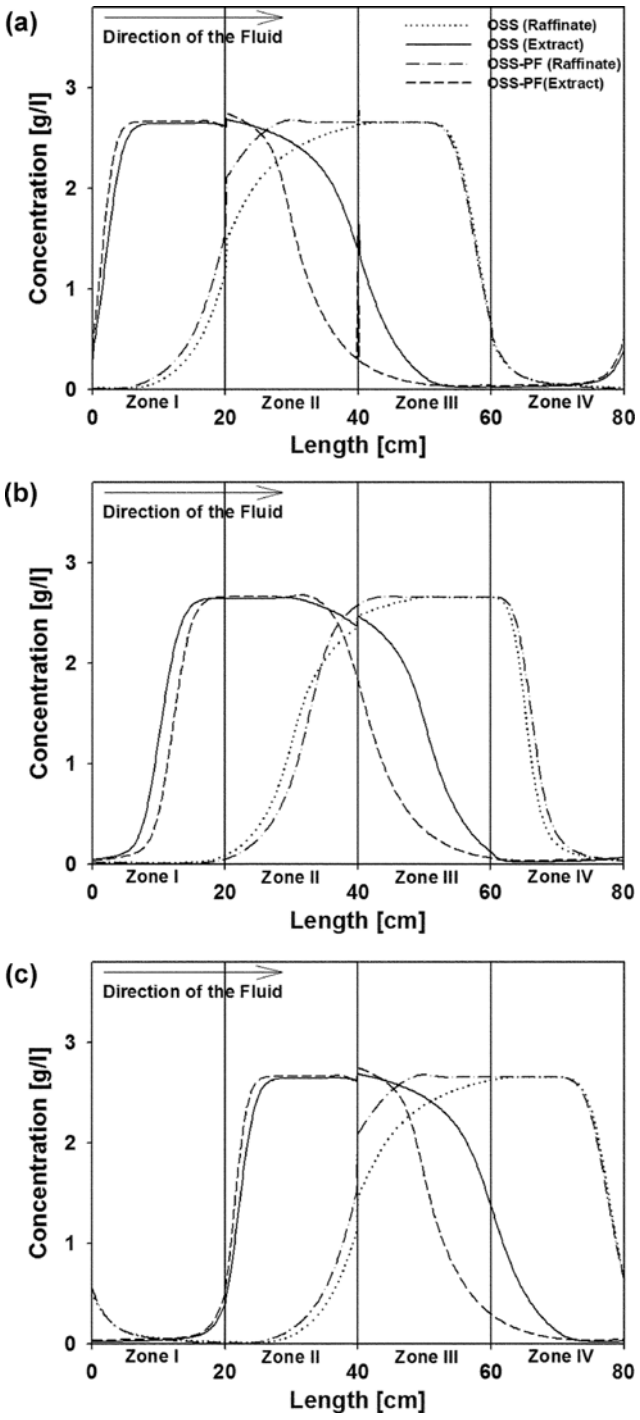

Fig. 7. Internal concentration profiles of the OSS (θ_{OSS}=0.5) and OSS-PF operation at ($\theta_{OSS\text{-}PF}$=0.5) at the (a) beginning of the switching period, (b) middle of the switching period, and (c) end of the switching period.

zone I, as shown in Fig. 5(c).

The raffinate tail in the profile at 0-40 cm during OSS-PF operation increased with column length at the beginning of the switching period (Fig. 5(a)) due to PF injection during step B and rapidly moved toward the fluid flow direction during step A due to the high flow-rate of zone II (Fig. 5(b)). On the other hand, the front profile of the extract (at 20-60 cm) steeply decreased due to the low flow-rate in zones II and III during step B. However, the leading edge of the extract profile in zone IV (60-80 cm) exhibited a slightly increased concentration due to the high flow in zone IV in step B. This result also stemmed from the expanded extract tail, as shown in Fig. 5. The product concentration under OSS-PF operation was higher than that in the conventional SMB during the production period, as shown in Fig. 6, which clearly demonstrated an improvement in purity under OSS-PF operation. During the extract production period in an extract node (Step B in Fig. 6(a)), the impurity concentration was high but did not yield a positive effect on product purity.

The comparison between the internal concentration profiles of OSS and OSS-PF operation at $\theta_{OSS}=\theta_{OSS\text{-}PF}$=0.5 are presented in Fig. 7. At the beginning and end of the switching period, the concentration profiles of OSS-PF were positioned to the left of those of OSS operation because the same quantity of feed required for OSS was injected during step B in OSS-PF through PF injection (Figs. 7(a) and (c)). During step A, the flow-rate in each zone under

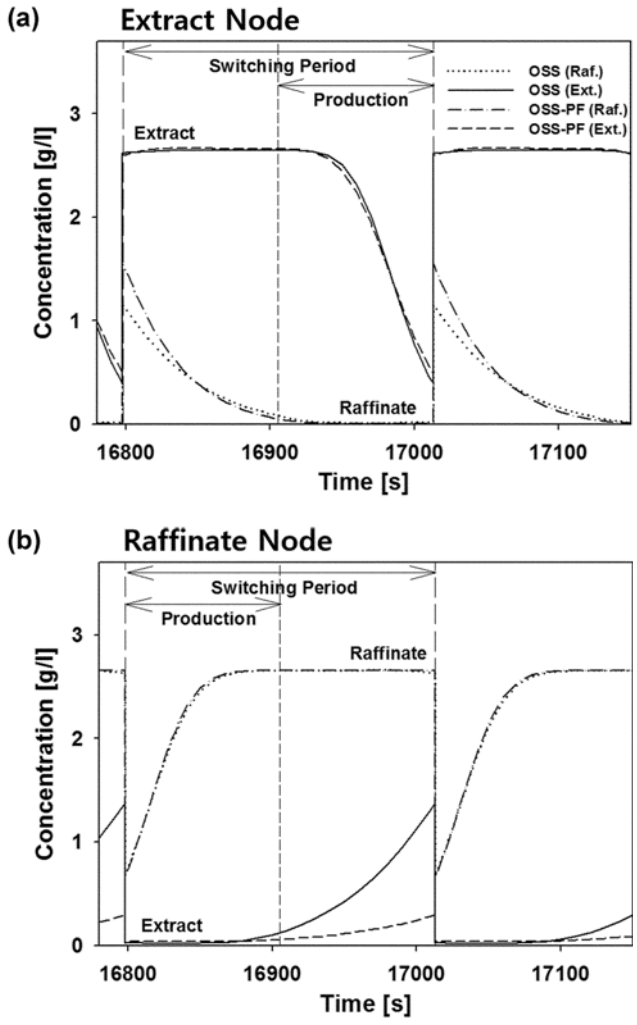

Fig. 8. Product concentration profiles of OSS (θ_{OSS}=0.5) and OSS-PF operation at ($\theta_{OSS\text{-}PF}$=0.5) at (a) the extract product node and (b) the raffinate product node.

OSS-PF operation was higher than that observed under OSS operation (Table 2). Therefore, the positions of the extract and raffinate profiles for OSS and OSS-PF operations changed, as shown in Fig. 7(b). Since the raffinate tail shifted more to the right side of zone II, it could contribute to improving extract purity under OSS-PF operation during step B.

However, the raffinate purity under OSS-PF operation was lower than that observed under OSS operation (Table 3) because the leading edge of the extract profile in zone III, which acted as a raffinate node impurity, was higher under OSS-PF operation during step A, as illustrated in Fig. 8. The difference between OSS and OSS-PF operations was only the feed injection method. Although the difference in impurity profiles between OSS and OSS-PF operations was observed especially in raffinated node (Fig. 8(b)), the difference in the concentration profile of main product between OSS and OSS-PF operations was small at each product node. Since the production period was the only important purity factor under OSS-PF operation, the smaller extract profile than that in OSS operation did not contribute to increased product purity. However, as shown in Fig. 8, the concentration profile difference between OSS and OSS-PF operation was small. Therefore, the main advantage of OSS-PF was improved purity under the maximum allowable operating flow-rate condition, which differed from OSS operation.

2. The Effect of Step Ratio

Fig. 9 presents the concentration profiles of each product node for OSS-PF operations at $\theta_{OSS\text{-}PF}$=0.25, 0.5, and 0.75. At the extract node, the impurity component (raffinate) was reduced as the step ratio decreased (Figs. 9(a), (c) and (e)). Thus, the extract purity improved when the operating strategy varied from OSS-PF4 ($\theta_{OSS\text{-}PF}$=0.75) to OSS-PF3 ($\theta_{OSS\text{-}PF}$=0.5), as shown in Table 3. However, as the production period increased, the extract product contained a larger quantity of contaminants, as shown in Fig. 9(a). Therefore, the extract purity deteriorated as the step ratio decreased (OSS-PF1, OSS-PF2, and OSS-PF3 in Table 3).

However, when a longer step A duration was used, the impurity component (extract) was reduced at the raffinate node (Figs. 9(b), (d) and (f)), resulting in an increased raffinate purity between OSS-PF1 ($\theta_{OSS\text{-}PF}$=0.25) and OSS-PF3 ($\theta_{OSS\text{-}PF}$=0.5). However, a longer production period led to a decrease in purity between OSS-PF3 ($\theta_{OSS\text{-}PF}$=0.5) and OSS-PF4 ($\theta_{OSS\text{-}PF}$=0.75) due to the same reasons affecting the extract node. As a result, OSS-PF operation at a moderate step ratio ($\theta_{OSS\text{-}PF}$=0.5) exhibited the highest separation performance at the selected operating point in this study. These results implied that the step ratio in OSS-PF operation functioned as an important factor in optimization of separation performance.

CONCLUSION

Outlet streams swing (OSS) operations can improve separation performance over conventional SMB operations. However, due to the increased flow rate in a specific zone, the OSS strategy can lead to a high pressure drop surpassing the acceptable pressure drop limit. To overcome this problem, OSS was combined with PF operation, denoted as OSS-PF operation. The separation behavior of OSS-PF operations was analyzed, and the potential of the developed strategy was demonstrated to improve the separation performance over conventional SMB operations under the same maximum flow rate limits at specific zones.

All performance parameters were improved under OSS-PF operation compared to the corresponding conventional SMB operation. Step ratio adjustments within a switching period were introduced as a new operating variable with regard to OSS-PF operation. Extracts were collected during the second stage of the switching period (step B), whereas less retained products (raffinate) were produced during the first stage (step A). To further limit the maximum flow rate, the feed was injected during the second stage of the switching period (step B). To improve the purity of both products (raffinate and extract), it is suggested that a moderate step ratio ($\theta_{OSS\text{-}PF}$=near 0.5) yields the most improved separation performance under OSS-PF operation. Additionally, if one product (raffinate or extract) is required, purity improvements could be easily achieved by controlling the step ratio under OSS-PF operations under the same flow-rate constraints as conventional SMB operation.

The OSS-PF strategy can provide a valuable engineering alternative toward improving the separation performance of the SMB

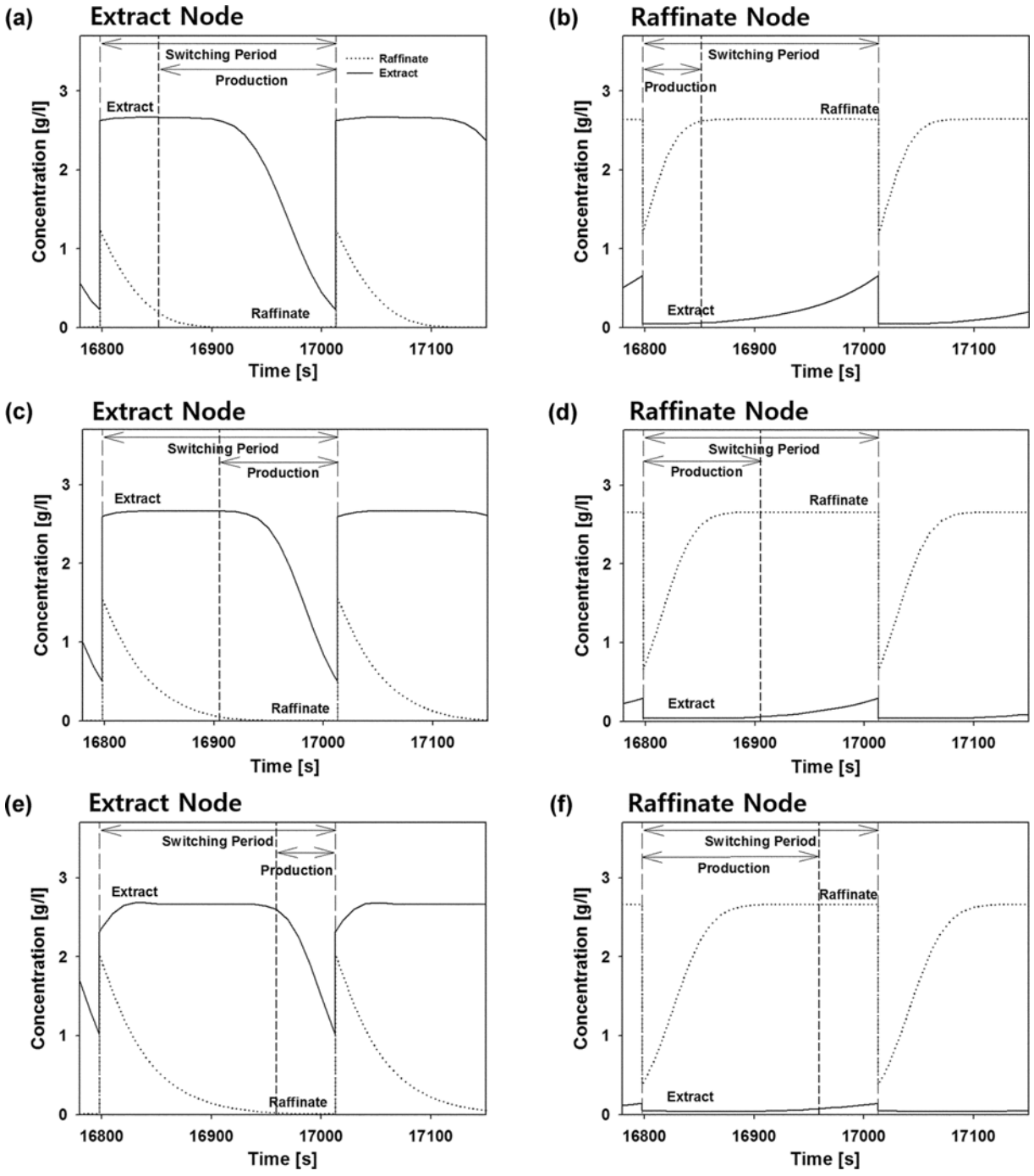

Fig. 9. Concentration profiles of product node in OSS-PF operation (a) Extract and (b) Raffinate at $\theta_{OSS\text{-}PF}$=0.25, (c) Extract and (d) Raffinate at $\theta_{OSS\text{-}PF}$=0.5, and (e) Extract and (f) Raffinate at $\theta_{OSS\text{-}PF}$=0.75.

process without exhibiting a significant pressure drop due to the increased flow-rate. Since an additional operating variable (step ratio) and constraints (allowable pressure drop and flow rate) are needed in the OSS-PF, further study is needed to optimize the operating parameters.

ACKNOWLEDGEMENT

We gratefully acknowledge the financial support from the DAPA/ADD of Korea and Converged Energy Materials Research Center in Yonsei University.

NOMENCLATURE

$C_{i,j}$: liquid phase concentration of component i in zone j [g/L]
$C_{i,j}^{out}$, $C_{i,j}^{in}$: concentrations of component i at the outlet and the inlet of zone j [g/L]
$\overline{C}_{i,E}$, $\overline{C}_{i,R}$: average extract and raffinate product concentrations [g/L]

D_L : axial dispersion coefficient in lumped kinetic model [cm^2/sec]
H_i : Henry's coefficient of component i [-]
L : length of the column [cm]
m_j : flow-rate ratio of each zone (j=I, II, III, and IV) [-]
N : number of theoretical plates of the column [-]
N_{column} : number of columns of the SMB system [-]
Q_j : flow rates through the corresponding zones j [mL/min]
Q_D, Q_E, Q_F, Q_R : desorbent, extract, feed, and raffinate flow rates [mL/min]
q^*, $q^*_{i,j}$: equilibrium concentration in the solid phase of component i in zone j [g/L]
t : time [sec; min]
t_{sw} : switch time; switching period [sec]
V : volume of column in SMB [cm^3]
z : length coordinate of the bed [cm]

Greek Letters

ε : overall void fraction (total porosity) of column [-]
μ : viscosity [Pa·s]
θ, $\theta_{OSS\text{-}PF}$, θ_{OSS} : step ratio of the OSS and OSS-PF operations [-]

Subscripts

D : desorbent
E : extract
F : feed
i (A, B) : solute
j : zones in SMB
R : Raffinate
Step A, Step B : step A and B in the OSS and OSS-PF operations

REFERENCES

1. J. A. Johnson and R. G. Kabza, in G. Ganetsos and P. E. Barker (Editors), *Preparative and Production Scale Chromatography*, Marcel Dekker, New York (1993).
2. N. V. D. Long, J. W. Lee, T.-H. Le, J.-I. Kim and Y.-M. Koo, *Korean J. Chem. Eng.*, **28**, 1110 (2011).
3. J. Lee, N. C. Shin, Y. Lim and C. Han, *Korean J. Chem. Eng.*, **27**, 609 (2010).
4. A. Rajendran, G. Paredes and M. Mazzotti, *J. Chromatogr. A*, **1216**, 709 (2009).
5. M. Schulte and J. Strube, *J. Chromatogr. A*, **906**, 399 (2001).
6. E. Lee, M. B. Park, J. M. Kim, W. S. Kim and I. H. Kim, *Korean J. Chem. Eng.*, **27**, 231 (2010).
7. Y.-S. Bae and C.-H. Lee, *J. Chromatogr. A*, **1122**, 161 (2006).
8. K.-M. Kim, H.-H. Lee and C.-H. Lee, *Ind. Eng. Chem. Res.*, **51**, 9835 (2012).
9. H. Schramm, A. Kienle, M. Kaspereit and Seidel-Morgenstern, *Chem. Eng. Sci.*, **58**, 5217 (2003).
10. K.-M. Kim and C.-H. Lee, *J. Chromatogr. A*, **1311**, 79 (2013).
11. H.-H. Lee, K.-M. Kim and C.-H. Lee, *AIChE J.*, **57**, 2036 (2011).
12. Y. Zang and P. C. Wankat, *Ind. Eng. Chem. Res.*, **41**, 2504 (2002).
13. J. K. Kim, N. Abunasser and P. C. Wankat, *Korean J. Chem. Eng.*, **22**, 619 (2005).
14. P. S. Gomes and A. E. Rodrigues, *Sep. Sci. Technol.*, **42**, 223 (2007).
15. K.-M. Kim, J.-Y. Song and C.-H, Lee, *J. Chromatogr. A*, **1340**, 79 (2014).
16. S. Mun, *Ind. Eng. Chem. Res.*, **49**, 9258 (2010).
17. S. Mun, *J. Chromatogr. A*, **1218**, 8060 (2011).
18. B. Sreedhar and Y. Kawajiri, *Chem. Eng. Sci.*, **116**, 428 (2014).
19. J.-Y. Song, D. Oh and C.-H. Lee, *J. Chromatogr. A*, **1403**, 205 (2015).
20. M. Mazzotti, G. Storti and M. Morbidelli, *J. Chromatogr. A*, **769**, 3 (1997).
21. G. Guiochon, S. G. Shirazi and A. M. Katti, *Fundamentals of Preparative and Nonlinear Chromatography*, Elsevier Academic Press, Boston, MA, 2nd Ed. (1994).
22. P. S. Gomes and A. E. Rodrigues, *Sep. Sci. Technol.*, **45**, 2259 (2010).
23. K. B. Lee, C. Y. Lim, Y. Xie, G. B. Cox and N.-H. L. Wang, *Ind. Eng. Chem. Res.*, **44**, 3249 (2005).
24. S. Ergun, *Chem. Eng. Prog.*, **48**, 89 (1952).
25. F. Charton and R.-M. Nicoud, *J. Chromatogr. A*, **702**, 97 (1995).